Int. J. Fuzzy Syst. (2020) 22(2):477–490
https://doi.org/10.1007/s40815-019-00741-8

Simulation of a Bubble-Column Reactor by Three-Dimensional CFD: Multidimension- and Function-Adaptive Network-Based Fuzzy Inference System

Erlin Tian[1] · Meisam Babanezhad[2] · Mashallah Rezakazemi[3] · Saeed Shirazian[4,5]

Received: 22 April 2019 / Revised: 8 August 2019 / Accepted: 16 September 2019 / Published online: 15 November 2019

Abstract Recently, novel approaches have been developed for simulating bubbly flow as well as distributed and constant phase evolution by means of a two-phase reactor. Among these approaches, the Eulerian–Eulerian method and soft computing approaches can be mentioned. Since complex numerical methods (for example, multidimensional Eulerian–Eulerian method) require several runs for fluid conditions optimization, a method which can decrease these runs can be very useful and practical. This method is provided by joining computational fluid dynamic (CFD) to the adaptive neuro-fuzzy inference system (ANFIS). In this technique, valuable information is provided for a careful analysis of fluid conditions. Also, it can facilitate a vast amount of data categorization in synthetic neural network nodes, which eliminates the need for a complex nonstructured CFD mesh. Moreover, a neural geometry can be provided, in which no limitation of mesh numbers in the fluid domain would exist. The key CFD parameters in the scale-up of the reactorstaken into consideration in the current research are gas and liquid circulations. These factors are applied as output factors for prediction tool in various dimensions in the ANFIS method. The results obtained in this study show appropriate conformity concerning ANFIS and CFD results depending on multiple dimensions. In this study, the grouping of CFD and multifunction the ANFIS method delivers the nondiscrete domain in different dimensions and presents an intelligent instrument for the local prediction of multiphase flow. The result shows that three inputs, which represent the dimension of the reactor, and learning stage of the ANFIS method provide a better understanding of flow characteristics in the two-phase reactor, while the two-dimensional ANFIS method even with multistructured functions cannot predict well the multiphase flow in the reactor.

Keywords Multidimensional machine learning · ANFIS method · Artificial intelligence method · Bubble-column reactor · CFD

✉ Saeed Shirazian
saeed.shirazian@tdtu.edu.vn

1 College of Computer and Communication Engineering, Zhengzhou University of Light Industry, Zhengzhou 450002, China

2 Department of Energy, Faculty of Mechanical Engineering, South Tehran Branch, Islamic Azad University, Tehran, Iran

3 Faculty of Chemical and Materials Engineering, Shahrood University of Technology, Shahrood, Iran

4 Department for Management of Science and Technology Development, Ton Duc Thang University, Ho Chi Minh City, Vietnam

5 Faculty of Applied Sciences, Ton Duc Thang University, Ho Chi Minh City, Vietnam

1 Introduction

Multiphase bubble-column reactors have widespread applications in different industries including chemical, biochemical, wastewater treatment, energy production, pharmaceutical where different liquids are required to mix more easily, aeration, and reaction concerning various elements [1]. The reason behind using bubble-column reactors (BCRs) compared to other kinds of reactors is that bubble-column reactors are considered to have more appropriate efficiency, rapid procedural operation, simple structure, and economic cleaning cost, etc., making them more favorable [2, 3]. Moreover, bubble-column reactors (BCRs) have proper efficiency in in-phase mixing properties and transferring rate amount [4]. Complex gas behavior moving inside the liquid phase of the bubble column plays an essential role in improving such reactors to gain more appropriate effectiveness. Simulating the hydrodynamic properties inside the column is a curiosity-arousing topic for research studies [5]. It is possible to model the liquid and gas flow dynamics near physical time and size by high-performance clusters. Various numerical methods can be applied for simulating multiphase flow patterns in the mentioned reactors [6, 7]. Nevertheless, there are some limitations which prevent the gas movement to achieve complete simulation through the stationary liquid. In addition, to measure the fluid flow at the operation time, high-speed microscopic cameras and smart probes are needed, thus making the process cost-prohibitive [8].

Recently computational fluid dynamics (CFD) [9, 10] methods have been used to model the multiphase fluid flow, including liquid and gas flow patterns inside bubble-column reactors [11–13]. Several investigations studied the effect of operational conditions on the hydrodynamics of bubble-column reactors by numerical methods [14, 15]. However, these methods are sometimes very time consuming when the correct interfacial force and turbulence models are required [16, 17]. For instance, for nonuniform bubbles with a high coalescence rate and break-up, the constant drag model is not suitable for modeling. Furthermore, the correct selection of turbulence models is very crucial to model fluid structure in the bubble-column reactor [18]. The addition of distinctive interfacial force and turbulence models increases the precision of CFD modeling but increases the computational time [19]. This issue is the main problem for the modeling of large bubble-column reactor when different operating conditions are required to observe the bubble-column performance [14].

In the review section, various soft computing approaches like neural networks, evolutionary algorithms, support vector machines, simulated annealing, along with integrated fuzzy system are proposed for the simulation [20, 21]. Artificial neural networks (ANN) [22, 23] or connectionist platforms are computing domains that are motivated by, but not fundamentally indistinguishable to, the biological neural meshes that frame animal brains. In this study, we specifically use ANN to learn the process engineering in order to have a high-performance training process. Among the methods, adaptive neuro-fuzzy inference system (ANFIS) [24, 25] can run the complicated simulations by utilizing a smart instrument to predict the complicated mechanisms in engineering [26]. For instance, in hazardous environments, controlling robotic movement is very useful for protecting people against the damages from chemical reactions [27–29]. Since the ANFIS method has intelligent behavior and comprehensive and complicated algorithms, it assists us in deciding different options.

Furthermore, the approach is capable of checking any accuracy errors. The ANFIS method can also learn the process with neuro-network, and for the prediction process, it uses the fuzzy inference platform. In this case, we have the advantage of utilizing neuro system only in the learning process, while decision part is carried out with a fuzzy overview. This method can be trained in several ways, including learning various inputs with one output [30]. The above-mentioned method is advantageous where a meaningful connection exists between all inputs and outputs. The simulated or experimental output data have a significant impact on the learning procedure. For the purpose stated, a suitable training output was carefully chosen to develop the ANFIS tool [31, 32].

The focus of the recent studies is on simulating the liquid and bubble interactions in a multiphase reactor by ANFIS [33]. Hydrodynamics data of multiphase reactor is applied for the training step according to these results. Moreover, integrating the macroscopic computational fluid dynamics and smart approach is a notable overview for calculating a different characteristic of BCRs. Furthermore, the algorithm can be an appropriate approach as an alternative for utilizing CFD methods for simulating bubble flow inside the BCR [34].

According to some studies, the distributed progression phase was simulated using an orifice, and the outcomes were then compared with the current volume-of-fluid method. It was found that for the estimation of the bubbly flow, the amount of regulations in the ANFIS method is a key factor [35, 36]. Nevertheless, to precisely predict the interface, an elevated fraction of the learning phase or the number of regulations is required.

In this research, the earlier method was utilized for simulating circulation in liquids and gases in various dimensions. A comparison was then drawn between the yields of the ANFIS method and the single size Eulerian–Eulerian method to indicate the capability of the intelligent algorithm and the research confirmation. In this study, we use the multidimensional ANFIS method with multistructured functions to predict the flow characteristics in the bubble-column reactor. The specific range of data in the bubble-column reactor is used for training, testing, and prediction process. The rest of the data are evaluated to observe the capability of method in the understanding of flow characteristics in the reactor.

2 Methodology

2.1 Related Works

Recently, the combination of CFD and ANFIS model has been used to predict the flow characteristics in the bubble-column reactor in several studies, as shown in Table 1.

Table 1 Recent development of ANFIS method in the field of bubble-column reactor

Ref.	Title	Objective	Remarks
[35]	Adaptive network-based fuzzy inference system analysis to predict the temperature and flow fields in a lid-driven cavity	Study on thermal analysis in the square cavity with a combination of CFD and ANFIS	ANFIS method can predict the flow pattern and thermal distribution in the cavity
[52]	A combination of computational fluid dynamics (CFD) and adaptive neuro-fuzzy system (ANFIS) for prediction of the bubble-column hydrodynamics	Validation of the ANFIS method in prediction of flow pattern in the 3D bubble-column reactor	There is a good agreement between CFD and ANFIS methods in prediction of gas–liquid interaction
[53]	Prediction of multiphase flow pattern inside a 3D bubble-column reactor using a combination of CFD and ANFIS	ANFIS prediction of flow pattern and bubble-column characteristics for different sparger sizes	The ANFIS method can predict different hydrodynamic parameters in the bubble-column reactor. In addition, this method can provide node-by-node mathematical expiration to predict outputs parameters as a function of input parameters
[54]	Liquid-phase chemical reactors: Development of 3D hybrid model based on CFD-adaptive network-based fuzzy inference system	ANFIS prediction of flow pattern and bubble-column characteristics for different column levels	This method can estimate different parameters at different levels regardless of CFD nodes
[30]	H_2-selective mixed-matrix membranes modeling using ANFIS, PSO-ANFIS, and GA-ANFIS	Tuning ANFIS parameters in prediction of flow pattern and bubble-column characteristics	Increasing number of inputs can improve the intelligence of method in the prediction of flow

2.2 Geometric Structure

To produce bubbly flow water with room settings, a 3D cylindrical BCR was applied. The ring sparger that had 20 orifices was then arithmetically employed in the base of the reactor; every single gas distributor orifices was 0.7 m, which produces very small bubbles with almost no interaction with other bubbles (almost zero coalescence rate). Also, the total superficial gas velocity, which equals 0.005 m/s in the BCR cross section, was produced by them [11]. In this study, an industrial bubble-column reactor model similar to Pfleger et al. is used [37].

2.3 CFD Modeling

For the liquid and gas flow simulation in the BCR, the Eulerian–Eulerian technique was performed via ANSYS CFX software. The momentum and continuousness shift equations for Eulerian–Eulerian methods can be written as [14]

$$\frac{\partial}{\partial t}(\rho_k \in_k) + \nabla(\rho_k \in_k u_k) = 0 \tag{1}$$

In the above equation, $\in_k$ and u_k denote the ratio and standard velocity of the continuous and dispersed phases, respectively.

The control volume approach was applied to find explanations regarding the conservation equations [9]. The estimates for the momentum change associated with the two phases of gas and liquid can be written as

$$\frac{\partial}{\partial t}(\rho_k \in_k u_k) + \nabla(\rho_k \in_k u_k u_k) = -\nabla(\in_k \tau_k) - \in_k \nabla p + \in_k \rho_k g + M_{I,k} \tag{2}$$

Three terms of stress, pressure gradient, and gravity are manifested by the momentum transfer equation. Furthermore, the interfacial momentum exchange during phase interaction between the continuous and dispersed phases is described by this equation [16–18]. The first term which is stress and presented by the momentum transfer equation for matrix and dispersed phase is as follows:

$$\tau_k = -\mu_{\mathrm{eff},k}\left(\nabla u_k + (\nabla u_k)^{\mathrm{T}} - \frac{2}{3} I(\nabla u_k)\right) \tag{3}$$

where μ_{L} denoted viscosity of the matrix phase, molecular function viscosity, or viscosity according to the bubble-induced turbulence:

$$\mu_{\mathrm{eff,I}} = \mu_{\mathrm{L}} + \mu_{\mathrm{T,L}} + \mu_{\mathrm{BI,L}} \tag{4}$$

The effective viscosity is calculated according to the effectual viscosity:

$$\mu_{\mathrm{eff,G}} = \frac{\rho_{\mathrm{G}}}{\rho_{\mathrm{L}}}\mu_{\mathrm{eff,L}} \tag{5}$$

The whole forcing scheme between gas and liquid fluids is given as

$$M_{\mathrm{I,L}} = -M_{\mathrm{I,G}} = M_{\mathrm{D,L}} + M_{\mathrm{TD,L}} \tag{6}$$

The drag force can be defined as follows:

$$M_{\mathrm{D,L}} = -\frac{3}{4} \in_{\mathrm{G}} \rho_{\mathrm{L}} \frac{C_{\mathrm{D}}}{d_{\mathrm{B}}} |u_{\mathrm{G}} - u_{\mathrm{L}}|(u_{\mathrm{G}} - u_{\mathrm{L}}) \quad (7)$$

In the above mentioned equation, d_{B} represents the bubble diameter and C_{D} denotes the drag coefficient.

For implementing a more effectual prediction of bubbly flow, the term of turbulent dispersion force was applied. The defining turbulent dispersion force linking the continuous and dispersed phases was modeled by Lopez de Bertodano et al. [38], which can be written as follows:

$$M_{\mathrm{TD,L}} = -M_{\mathrm{TD,G}} = -C_{\mathrm{TD}} \rho_{\mathrm{L}} k \nabla \in_{\mathrm{L}} \quad (8)$$

where C_{TD} and k specify the liquid turbulent dispersion coefficient and turbulent kinetic energy (TKE), respectively.

Turbulence shaping is required to precisely model the bubbly flow. Thus, when turbulence actions are present, an improved inspection of gas motion is obtained.

$$\mu_{\mathrm{T,L}} = \rho_{\mathrm{L}} C_{\mu} \frac{k^2}{\varepsilon} \quad (9)$$

The kinetic energy and the rate of energy dissipation are in harmony with Tabib et al. [14].

2.3.1 Grid

In this study, in order to generate the mesh structure for the calculation of fluid flow by Eulerian–Eulerian technique, the nonuniform mesh structure was utilized. This structure was almost similar to Laborde-Boutet et al. [39].

2.4 Integration of Neuro-Fuzzy Mechanism

2.4.1 Neuro-Fuzzy Calculating

This method is considered as an intelligent tool for building systems for the calculation of soft computing, which creates computational or mathematical conceptions by altering linguistic ideas [40, 41]. Furthermore, it can alter its manner in circumstance deviations. Hence, it can compute the behavior of sequences referring to doubtful procedures. One of the advantages of this method is the application of computing techniques in an active process rather than applying one specific process followed by merely one computing approach. The development of hybrid intelligent systems can be acquired by finding such computing technologies, for example, the neuro-fuzzy computing made actually like the outcome of intelligent systems construction [42]. The system patterns are first identified by the method via neural networks and afterward, fuzzy inference systems based on the identification of the previous patterns. Finally, a fascinating and efficient technique can be built with the assistance of utilizing the two methodologies simultaneously, to identify and anticipate a difficulty. Therefore, it can pick up from physical complications plus altering its manner each time the condition varies [43, 44].

2.4.2 ANFIS

The fuzzy logic structures can create computational and mathematical conceptions by transferring linguistic ones

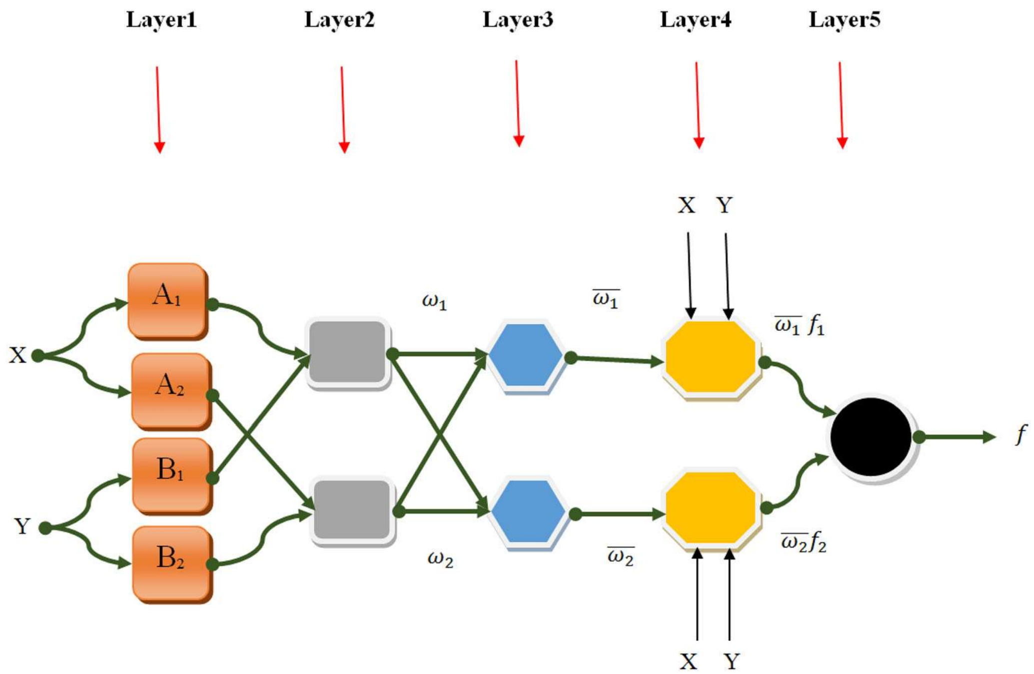

Fig. 1 Adaptive neuro-fuzzy inference system pattern that is utilized to simulate gas hold-up and various input data

[45, 46]. Nevertheless, there is a limitation by which the boundary conditions change, since their physical processes of learning and detection do not occur accurately [47, 48]. However, by combining ANN and fuzzy logic methodologies, it is possible to develop both the educating procedure and the uncovering capability which is called ANFIS combining. The method refers to learning characteristics of neural networks and the usual language description of fuzzy systems. In the current study, we utilize the fuzzy inference structure. The system consists of two input parameters in the BC, which are *y* and *x*, and one output parameter *z*, which is the fuzzy learning replication that was first designated for the ANFIS. Broadly speaking, three types of fuzzy representations exist: Sugeno, Mamdani, and Tsukamoto.

The membership calculation structures at the smart outputs are either constant or linear in the Sugeno model compared with the Mamdani model. The final system applied fuzzy system since it does not have as much model transparency and computational time. Therefore, it is applied in the ANFIS framework to model the

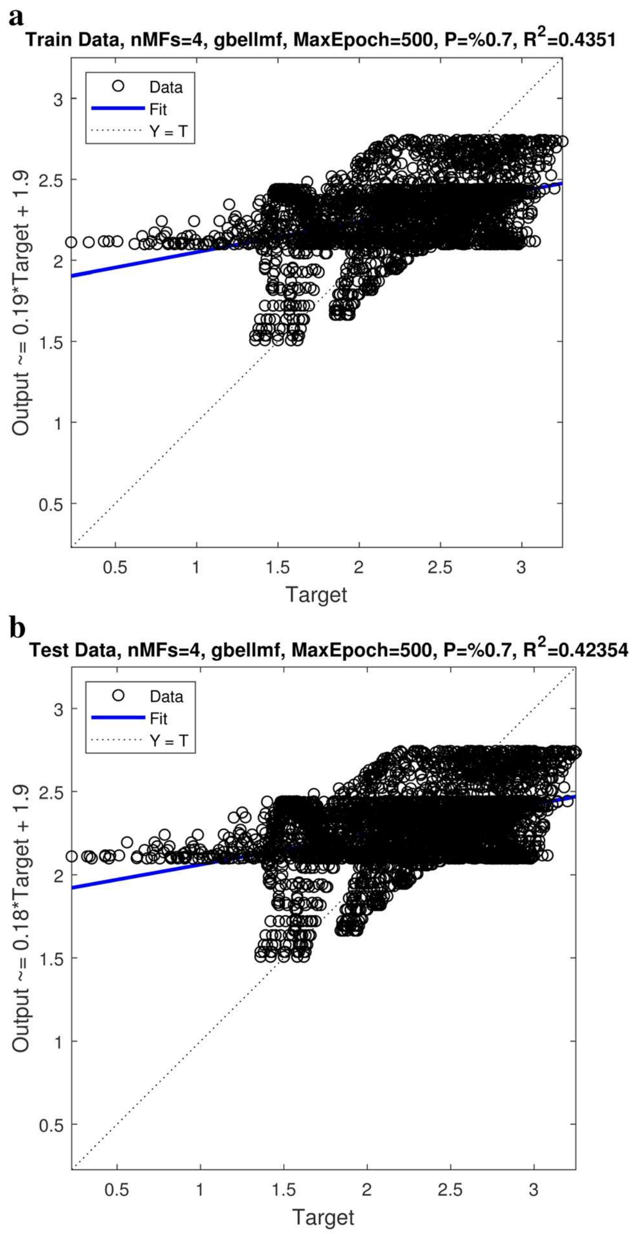

Fig. 2 **a** Training authentication of amount of gas in the multiphase reactor with 4000 data in the 1D ANFIS (*x*-position). **b** Testing authentication of amount of gas in the multiphase reactor with 4000 data in the 1D ANFIS (*x*-position)

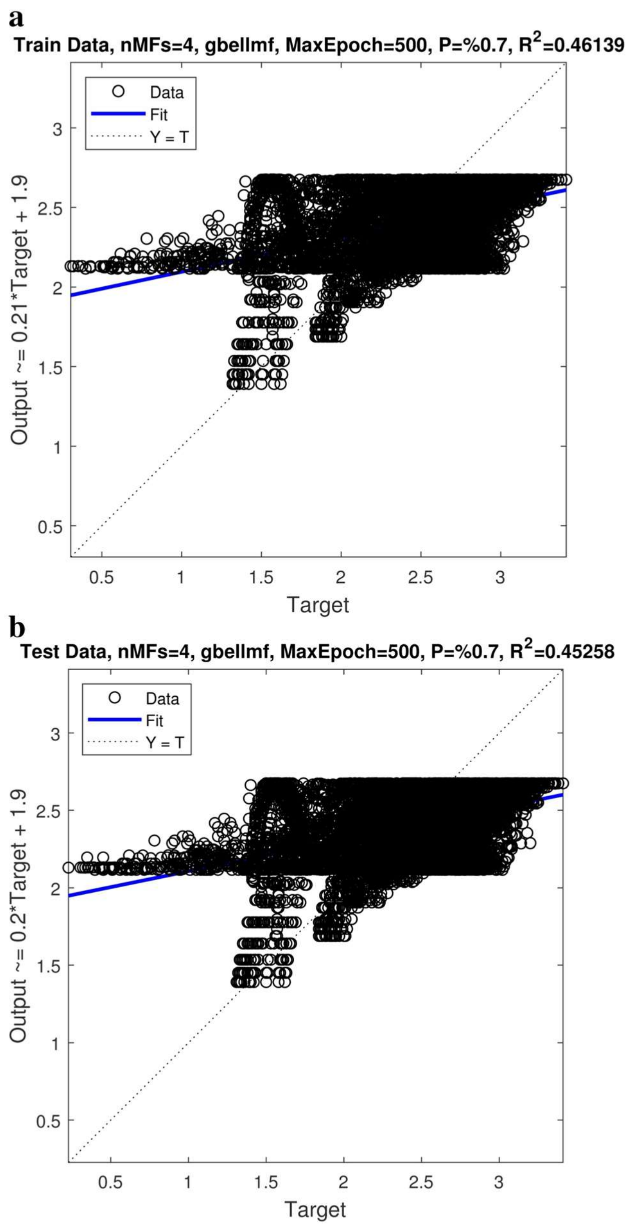

Fig. 3 **a** Training authentication of amount of gas in the multiphase reactor with 8000 data in the 1D ANFIS (*x*-position). **b** Testing authentication of amount of gas in the multiphase reactor with 8000 data in the 1D ANFIS (*x*-position)

complex problems with speedy and nonlinear behavior [36, 49].

We can suggest the first-order Sugeno fuzzy model as a unique category of fuzzy systems. Furthermore, the model has a wide application for fuzzy control systems for prediction of physical complications. It possesses excellent talent in learning and describing the problem referring to membership functions of input data, which is considered as the advantage of this model [50].

In this research, the first-order Sugeno fuzzy structure is applied, consisting of two fuzzy if–then regulations as shown below:

$$\text{Rule 1: if } x \text{ is } A_1 \text{ and } y \text{ is } B_1,\ \text{then } f_1 = p_1x + q_1y + r_1 \tag{10}$$

$$\text{Rule 2: if } x \text{ is } A_2 \text{ and } y \text{ is } B_2,\ \text{then } f_2 = p_2x + q_2y + r_2 \tag{11}$$

Figure 1 represents the reasoning calculations of this Sugeno structure. There are almost the same functions for the same layer in each node. The ith node output in layer 1 is represented as O_i^1.

Layer 1 can be defined as follows:

Every node i is an integrated node in this first layer and consists of nodes designated as follows:

$$O_i^1 = \mu_{A_i}(x)$$

also, y or x is the input parameter to node A_i; moreover,i or B_{i-2} is a connected linguistic structure. A fuzzy structure calculation is entirely described by means of its membership function including trapezoidal, triangular, Gaussian, sigmoidal, and generalized bell. Trapezoidal and triangular functions consist of the straight-line division, but the problem with them is that the corner points are not smooth, which the parameters denote. Nevertheless, these criteria are met by the other functions. Two aspects of these functions are extensively known, namely, figures and probability. The bell function consists of one more degree of freedom since it contains one extra parameter compared with the Gaussian function. Hence, it can adjust the steepness in the crossover points. Since the generalized bell function has great abilities to generalize the nonlinear parameters, it was applied in this study:

$$\mu_A(x) = \frac{1}{1 + \left[\left(\frac{x - c_i}{a_i}\right)^2\right] b_i} \tag{12}$$

In this relation, $\{c_i, b_i, a_i\}$ is the parameters set. The bell-shaped calculation varies according to the variation of the parameters.

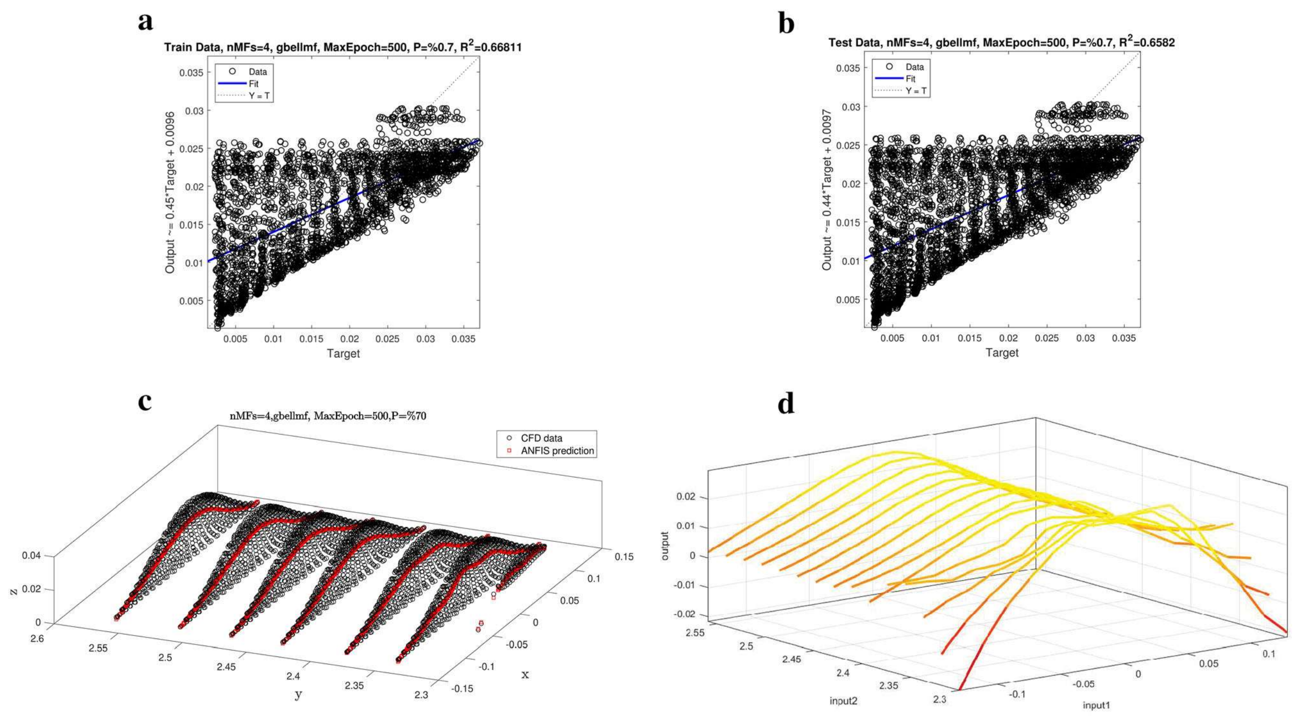

Fig. 4 **a** Training authentication of amount of gas in the multiphase reactor with 4000 data in the 2D ANFIS (y- and x-positions). **b** Testing authentication of amount of gas in the multiphase reactor with 4000 data in the 2D ANFIS (y- and x- positions). **c** Comparison of ANFIS and CFD processesfor predicting the amount of gas in the multiphase reactor with 4000 of data in the 2D ANFIS (x- and y-directions). **d** Prediction of amount of gas in the multiphase reactor with 4000 data in the 2D ANFIS (input 1 = x-direction, input 2 = y-direction)

Layer 2 is defined as follows: each node in this section is an unchanging one, and the output results concerning it is the consequence of the whole incoming section signals:

$$w_i = \mu_{A_i}(x) \times \mu_{B_i}(y), \quad i = 1, 2. \tag{13}$$

Layer 3 can be described as follows: Each node in this part is an unchanging one. The ith node structure calculates the firing strength proportion of the ith law to the total of the firing strengths of the entire laws:

$$\overline{w_i} = \frac{w_i}{w_1 + w_2}, \quad i = 1, 2. \tag{14}$$

For convenience, this specific layer's outputs are named firing strengths.

Layer 4 each node present in the 4th layer has a node structure and is an adaptive node:

$$O_i^4 = \overline{w_i} f_i = \overline{w_i}(p_i x + q_i y + r_i) \tag{15}$$

where $\overline{w_i}$ is defined as a strength structure corresponding to the previous layer.

Layer 5 can be defined as follows: In this structure, the single size node is considered as a constant node section. Hence, it calculates the entire output in lieu of the summation of all the incoming signals:

$$O_i^5 = \text{overall output} = \sum \overline{w_i} f_i = \frac{\sum w_i f}{\sum w_i} \tag{16}$$

Several variables of the ANFIS constructions are determined by means of an approach, which is called the integrated learning process. In the forward pass section, signals travel in the direction of the succeeding layers up to the point of reaching Layer 4. This method is limited within the range of data that we use during the training process, and if the flow regime is changed from homogeneous to heterogeneous flow pattern, then the method cannot correctly estimate the overall behavior of the flow. Therefore, we always need to learn the process engineering in one

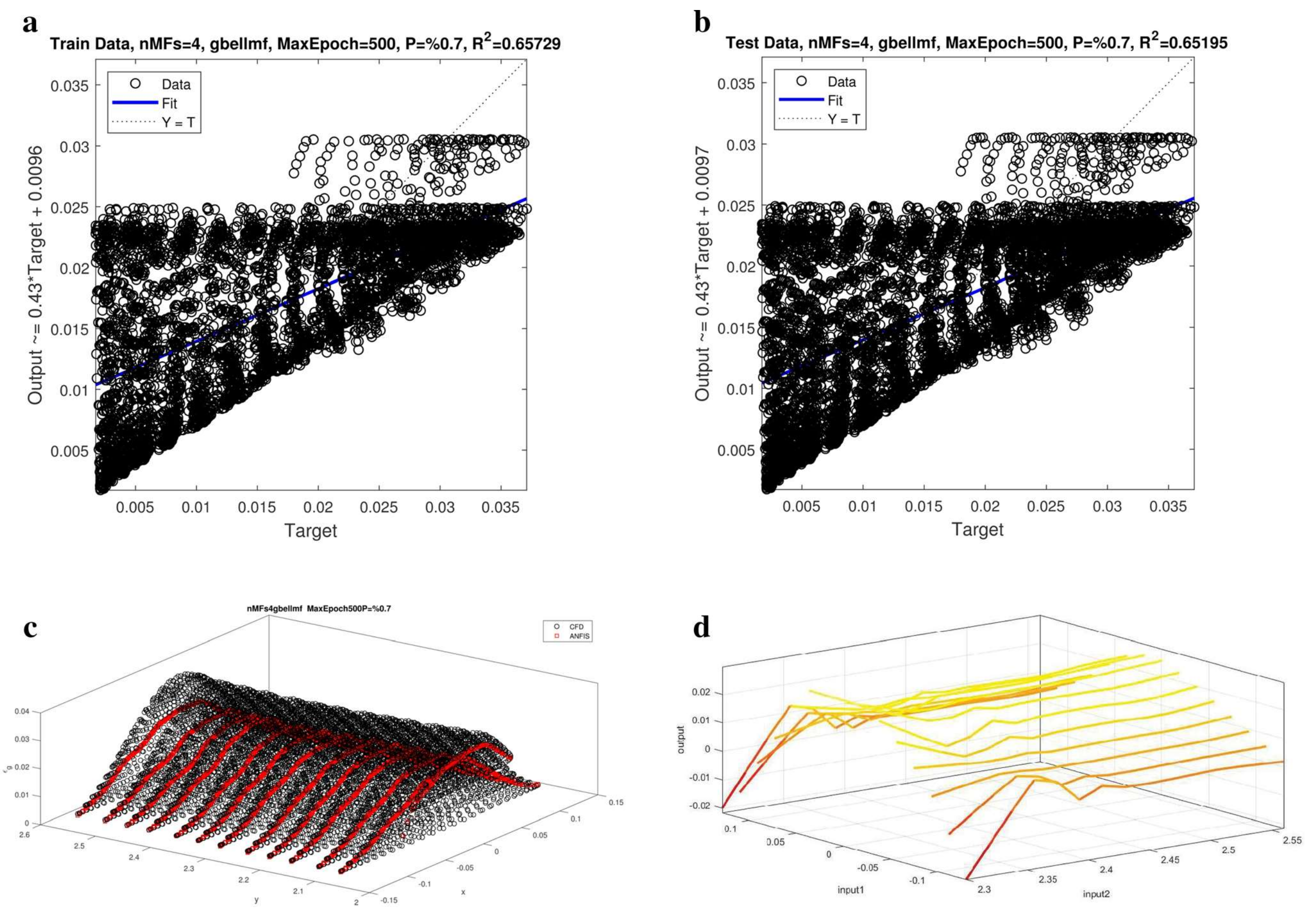

Fig. 5 **a** Training authentication of the amount of gas in the multiphase reactor with 8000 data in the 2D ANFIS (y and x positions). **b** Testing authentication of amount of gas in the multiphase reactor with 8000 data in the 2D ANFIS (y- and x positions). **c** Comparison of ANFIS and CFD techniques to predict the amount of gas in the multiphase reactor with 8000 data in the 2D ANFIS (x and y directions). **d** Prediction of amount of gas in the multiphase reactor with 8000 data in the 2D ANFIS (input 1 = x direction, input 2 = y direction)

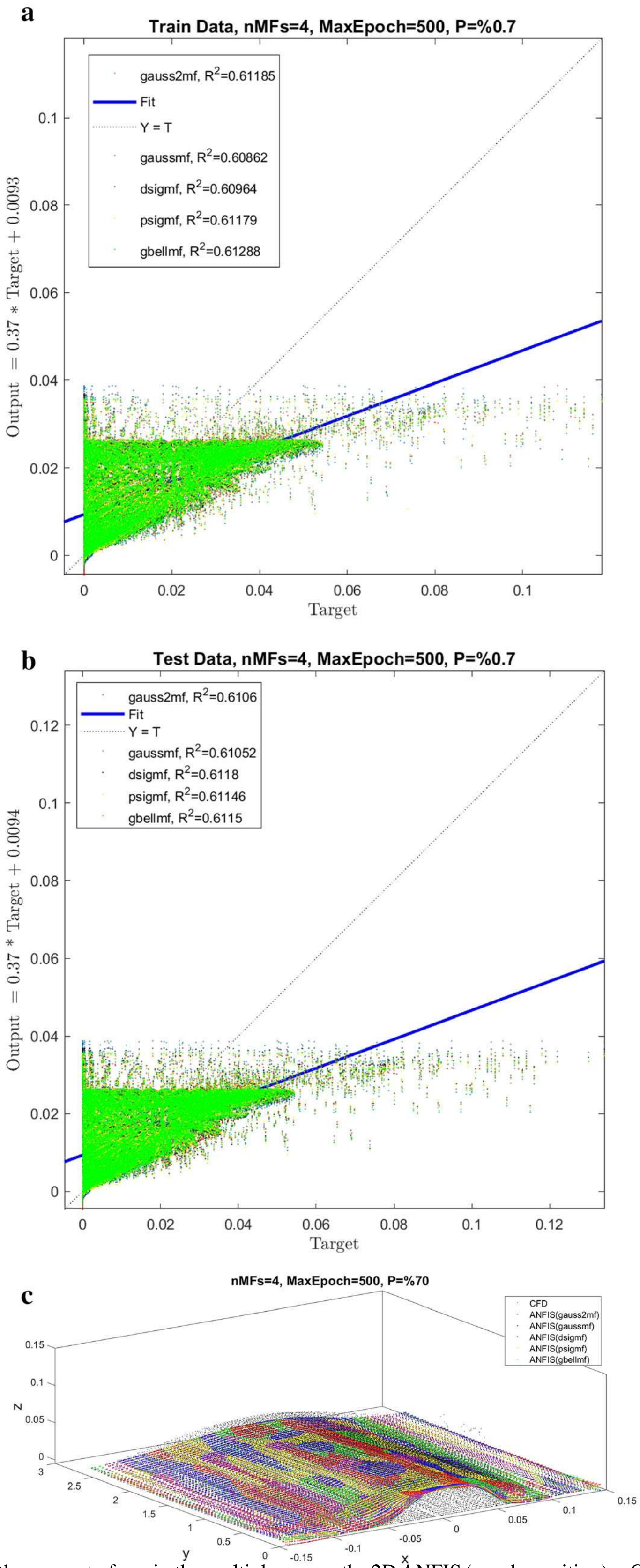

Fig. 6 **a** Training confirmation of the amount of gas in the multiphase reactor with different types of MFs with 43005 data in the 2D ANFIS (*y* and *x* positions). **b** Examination of authentication for the amount of gas in the multiphase reactor with different types of MFs with 43005 data in the 2D ANFIS (*y* and *x* position). **c** Comparison of the CFD method with different types of MFs in the ANFIS technique for forecasting the amount of gas in the multiphase reactor with 43005 data in 2D ANFIS (*x* and *y* direction)

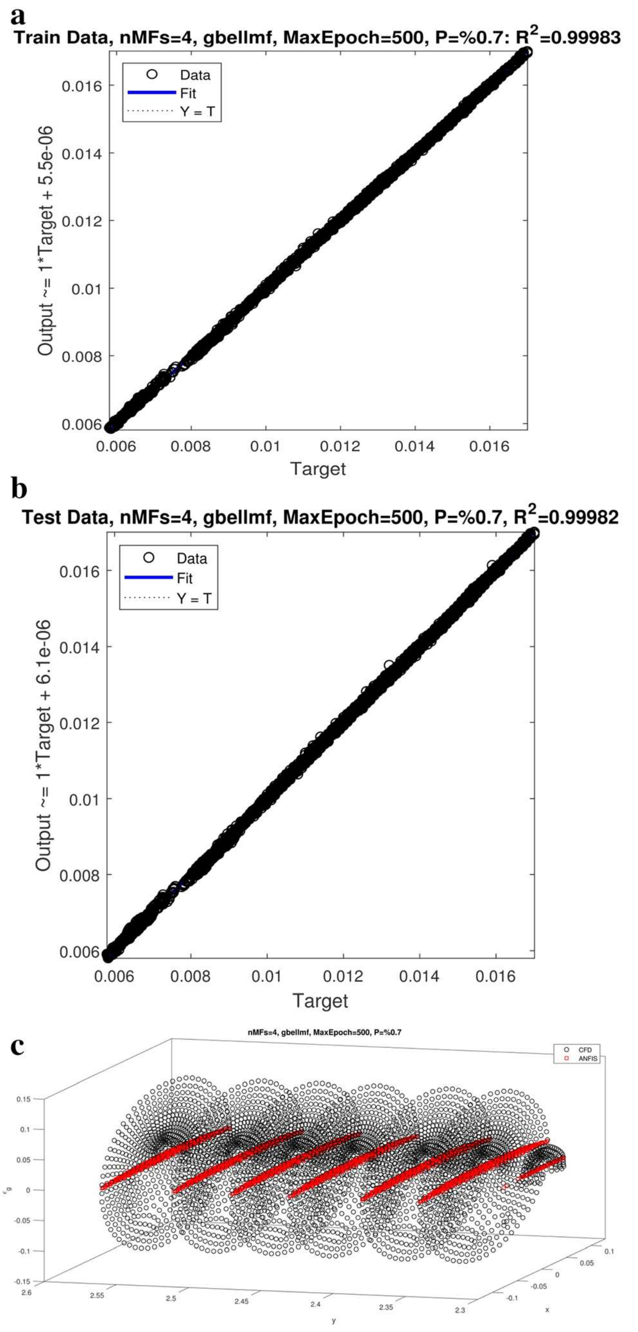

Fig. 7 **a** Training confirmation of amount of gas in the multiphase reactor with 4000 data in 3D ANFIS (y, x, and z placements). **b** Testing confirmation of amount of gas in the multiphase reactor with 4000 data in 3D ANFIS (y, x, and z placements). **c** Comparison of ANFIS and CFD techniques for forecasting the amount of gas in the multiphase reactor with 4000 data in 3D ANFIS (x and y directions)

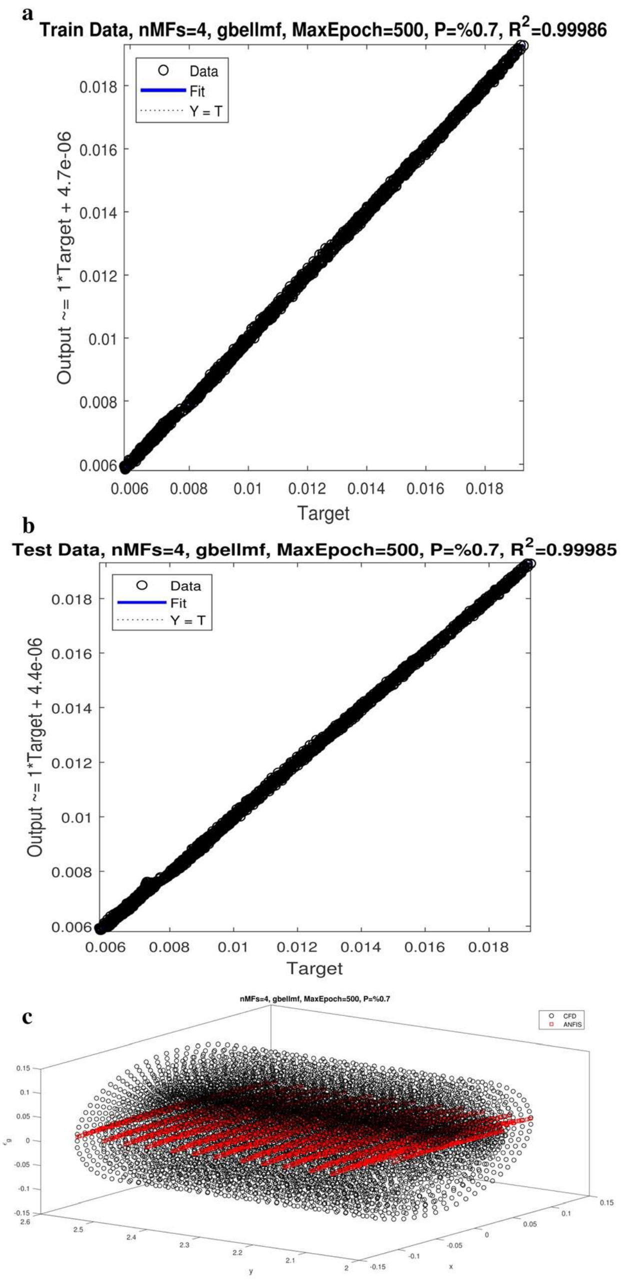

Fig. 8 **a** Training confirmation of amount of gas in the multiphase reactor as delay with 8000 data in 3D ANFIS (y, x, and z placements in BC).**b** Testing validation of amount of gas in the multiphase reactor with 8000 data in 3D ANFIS (y, x, and z placements). **c** Comparison of ANFIS and CFD techniques for the amount of gas in the multiphase reactor with 8000 data in 3D ANFIS (x and y directions). **d** Forecasting the amount of gas in the multiphase reactor with 8000 data in 3D ANFIS (input 1 = x direction, input 2 = y direction, input 3 = z direction)

regime and avoid transient from laminar to turbulent regime. In addition, this model cannot accurately predict the interface between dispersed and continuous phases, in case of having interface modeling, such as the volume-of-fluid method (VOF) [51]. In this case, we need to increase the number of rules and number of inputs affecting the computational time.

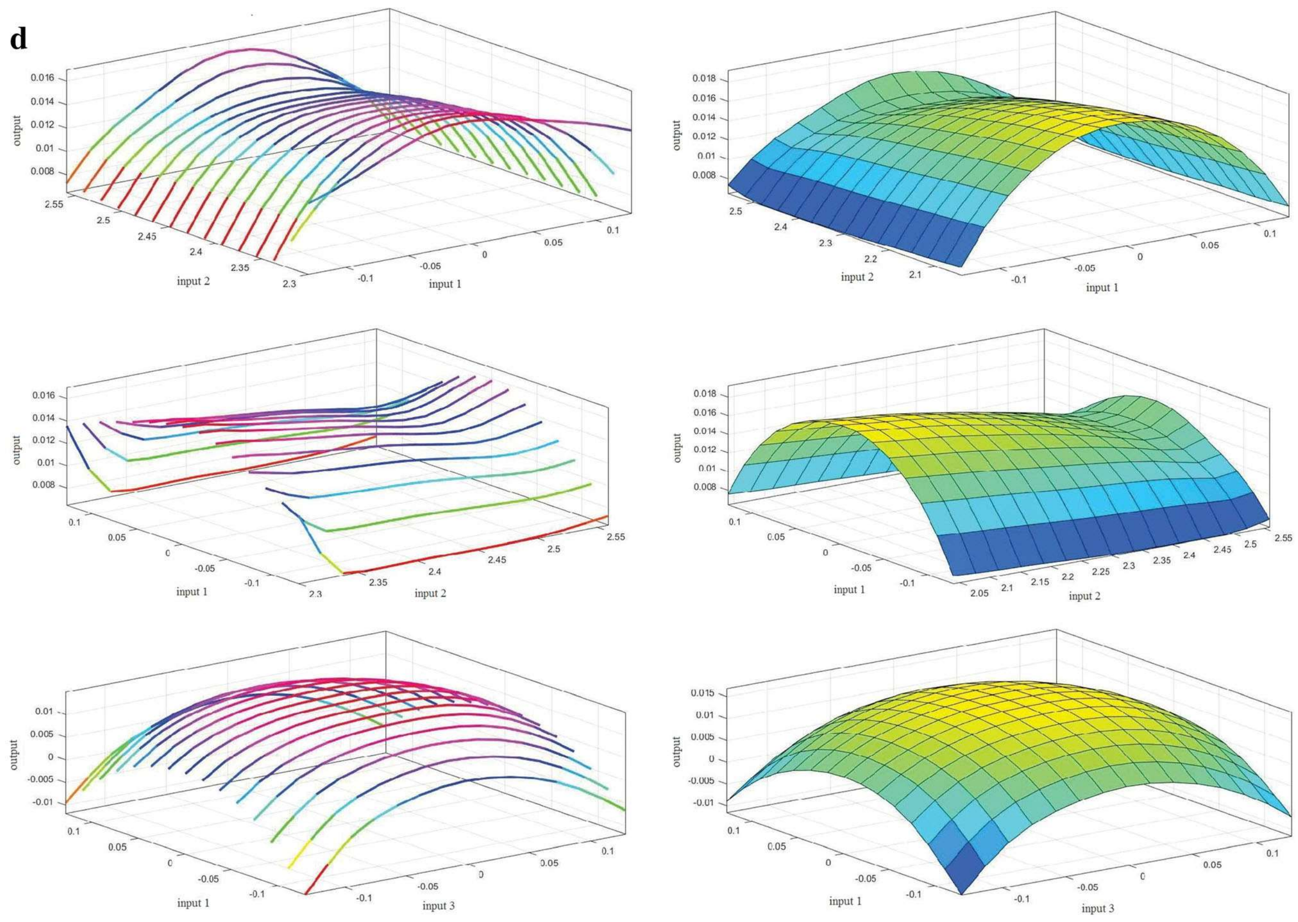

Fig. 8 continued

3 Results and Discussion

In this research, a cylindrical bubble-column reactor was simulated using the CFD method, and CFD findings were used for the training procedure. In the learning process of CFD data, there was no noise on the data, which was an advantage of CFD data and enabled us to learn all data without filtering or using denoiser machine learning algorithms. To understand the behavior of the method in the prediction of flow pattern, we define the criteria for the intelligence of the ANFIS method. In this case, we can observe when exactly, this method can cover the whole bubble-column reactor. In the training process first, we got 70% of aggregate data, and by changing the number of input parameters, we checked the overall error in the ANFIS prediction. Since with the increasing number of inputs, the performance of the ANFIS method increased in terms of accuracy, we used the maximum number of inputs during the training process. After deciding on the accurate platform for the prediction of the flow, we migrated to the testing stage and added the rest of the testing data to compare with the ANFIS method. In this part, as we dealt with "not existing data" during the training process, we can observe the overall ability of the method in the estimation of the flow pattern in the column. In the testing process (validation part), we evaluated the regression, and the errors between prediction results of CFD and ANFIS methods. As multivariable input results can significantly change the behavior of the smart method (ANFIS), we selected a different level of data from the bubble-column reactor. For training process, 9.3% of total data was selected at the beginning, and after the first training and evaluation (testing of data), we chose 18.6% of the total data from the top of the column. In general, during the training process, 70% of data was selected, and after the learning process, the rest of the data (30%) was added to the dataset for comparison. To understand ANFIS behavior, we selected a set of data which was collected from the top of the column and based on randomized algorithms. We studied the collected data. This way of data collection enabled us to eliminate the effect of initializing condition on the learning process, and the method can only compare data based on the complexity of data from top to bottom. The prediction results show that more data in the training

Table 2 ANFIS training parameters and errors

	Number of inputs	Number of MFs	Number of data	Type of MFs	Max epoch	P (%)	Training R^2	Testing R^2	Training mean error	Testing mean error	Training STD error	Testing STD error	Training MSE	Testing MSE	Training RMSE	Testing RMSE
1	1 (x)	4	4000	Gbellmf	500	70	0.4351	0.42354	4.3172e−09	− 0.0099	0.4451	0.4534	0.1980	0.2057	0.4450	0.4535
2	1(x)	4	8000	Gbellmf	500	70	0.46139	0.45258	1.9195e−09	0.0019	0.4564	0.4574	0.2082	0.2092	0.4563	0.4574
3	2 (x and y)	4	4000	Gbellmf	500	70	0.66811	0.6582	5.9345e−10	− 4.7111e−5	0.0074	0.0075	5.5065e−5	5.5838e−5	0.0074	0.0075
4	2 (x and y)	4	8000	Gbellmf	500	70	0.65729	0.65195	1.2730e−10	− 7.7574e−06	0.0076	0.0076	5.7239e−5	5.7237e−5	0.0076	0.0076
5	2 (x and y)	4	43,005	Gauss2mf	500	70	0.61185	0.6106	− 6.997e−12	2.3303e−05	0.0113	0.0113	1.2855e−04	1.2912e−04	0.0113	0.0113
6	2 (x and y)	4	43,005	Gaussmf	500	70	0.60862	0.61052	4.5690e−12	3.5128e−05	0.0114	0.0114	1.3064e−04	1.2914e−04	0.0114	0.0114
7	2 (x and y)	4	43,005	Dsigmf	500	70	0.60964	0.6118	7.2129e−12	3.7227e−05	0.0114	0.0113	1.3038e−04	1.2881e−04	0.0114	0.0113
8	2 (x and y)	4	43,005	Psigmf	500	70	0.61179	0.61146	7.38e−12	− 2.43e−05	0.0113	0.0113	1.2925e−04	1.2890e−04	0.0113	0.0113
9	2 (x and y)	4	43,005	Gbellmf	500	70	0.61288	0.6115	1.2682e−11	2.3514e−05	0.0113	0.0114	1.2829e−04	1.2889e−04	0.0113	0.0114
10	3 (x, y and z)	4	4000	Gbellmf	500	70	0.99983	0.99982	3.3650e−10	− 1.9412e−07	5.0418e−05	5.1281e−05	2.5411e−09	2.6291e−09	5.0409e−05	5.1275e−05
11	3 (x, y and z)	4	8000	Gbellmf	500	70	0.99986	0.99985	2.9855e−10	− 1.4792e−07	5.4584e−05	5.6909e−05	2.9789e−09	3.2382e−09	5.4579e−05	5.690e−05

of the ANFIS method can provide a better understanding of the intelligent approach. In addition to the different levels of training, we set the algorithm to learn from different dimensions or based on various inputs. In this study, one dimension represents x coordinate as input and the amount of gas as output. The two-dimensional (2D) modeling learns data in y- and x-directions, and the output is the amount of gas hold-up. The three-dimensional (3D) ANFIS method demonstrates modeling for x-, y-, and z-directions as inputs, and the output is the gas hold-up.

When the input parameter is x, and the output is a gas hold-up, the training and testing processes are not accurate and the $R^2 < 0.5$ (Fig. 2a, b). This process of evaluation is examined for different amounts of data such as 9.3 and 18.6%. By increasing the number of data up to 18.6%, the ANFIS method cannot reach to the intelligence level in the learning and testing processes (Fig. 3a, b).

To learn more about the influence of the dimension of the method, we added the second input (y), and in this case, we trained a set of data with two inputs and one output as a gas delay. The findings indicate that we achieved better agreement between CFD and ANFIS results when one more input is added to the learning process ($R^2 > 0.6$) (Fig. 4). In the case of increasing number of meshes in the learning process up to 18.6%, we observed that there was a marginal difference between the ANFIS and CFD data. In other words, the method cannot achieve better accuracy, when the number of data increases (Fig. 5).

To see the consequence of membership function for the accurateness of the ANFIS method, we examined different functions on the accuracy of the technique for 100% of data. Figure 6 shows the influence of the membership function for the accurateness of the technique for the full bubble-column reactor. The results show that all functions cannot change the main accuracy of the method and almost the R^2 is about 0.61. Results represent that for training, testing, and prediction process, the accuracy of the method is almost similar for different functions.

Since the bubble-column reactor's inner gas flow is meaningful when the domain is three dimensional, we select three inputs which are x, y, and z coordinates and one output (gas hold-up). The results show that by increasing the number of inputs, the ANFIS model can significantly improve its own accuracy and R^2 is about 0.99 (Fig. 7). This significant agreement is constant when the number of data increases (Fig. 8). The computational time for a higher value of R^2 in the learning process is 2.26 e+03 s, while this model can predict the process in 2.82 s. After training and testing, we create the neural nodes and predict the gas hold-up based on new mesh domain. This new mesh structure is independent of the physical or numerical conditions. Table 2 shows that the increment in input parameters significantly affects the intelligence of the system. In this case, R^2 is about 0.999, and all error characteristics, such as (mean error, STD error, MSE, and RMSE) are very minimal in the training and testing processes.

4 Conclusions

This research represents multiple dimensions of ANFIS method as multilevel training process, which is interesting and important to deal with the analysis of fluid geometry. Regarding geometry analysis, principally, multiphase fluid flow can be solved, and fluid parameters can be optimized at different levels of the reactor. This analysis enables learning from every CFD mesh indicating resident learning model as well as presenting the findings in neural network nodes, which is totally self-governing from the CFD procedures and complex mesh analysis.

As the flow pattern in the bubble-column reactor is fully defined in 3D and 2D predictions of bubbly flow, we cannot capture all flow structure and time averaging; we consider 3D CFD study of bubble-column reactor. Optimization of 3D fluid parameters requires a significant amount of time and cost. Hence, the ANFIS method is considered as an excellent tool for the numerical method for optimizing few case studies without performing those conditions required under CFD methods. It is also possible to mesh refining with small computational time by this approach. This study indicates the application of training for the ANFIS method in various dimensions to create a self-governing technique to learn and predict. The huge agreement between the CFD and the ANFIS methods indicates that smart algorithm can be an alternative candidate for the conventional numerical method which requires high computational time. The ANFIS method can reach the understanding level of up to 8% of total data when particularly three geometric inputs are used for the learning process. However, two inputs with various functions is not an appropriate way to feed the ANFIS process to forecast the gas flow in the column. For further development of this work, there is a possibility to map the output parameters of the CFD method with the experimental study, which is helpful for a better understanding of the experimental and numerical parameters together. The online learning process is also feasible with the ANFIS method, while we have an active learning process for CFD method. In this case, AI can learn from numerical methods, and it can use this understanding of parameters for the online learning process.

Acknowledgements E. Tian acknowledges the Grant under NSFC: 61702462.

References

1. Sobrino, C., Acosta-Iborra, A., Izquierdo-Barrientos, M.A., De Vega, M.: Three-dimensional two-fluid modeling of a cylindrical fluidized bed and validation of the maximum entropy method to determine bubble properties. Chem. Eng. J. **262**, 628–639 (2015)
2. Rezakazemi, M., Razavi, S., Mohammadi, T., Nazari, A.G.: Simulation and determination of optimum conditions of pervaporative dehydration of isopropanol process using synthesized PVA–APTEOS/TEOS nanocomposite membranes by means of expert systems. J. Membr. Sci. **379**, 224–232 (2011)
3. Silva, M.K., d'Ávila, M.A., Mori, M.: Study of the interfacial forces and turbulence models in a bubble column. Comput. Chem. Eng. **44**, 34–44 (2012)
4. Díaz, M.E., Iranzo, A., Cuadra, D., Barbero, R., Montes, F.J., Galán, M.A.: Numerical simulation of the gas–liquid flow in a laboratory scale bubble column: influence of bubble size distribution and non-drag forces. Chem. Eng. J. **139**, 363–379 (2008)
5. Rabha, S., Schubert, M., Hampel, U.: Intrinsic flow behavior in a slurry bubble column: a study on the effect of particle size. Chem. Eng. Sci. **93**, 401–411 (2013)
6. Şal, S., Gül, Ö.F., Özdemir, M.: The effect of sparger geometry on gas holdup and regime transition points in a bubble column equipped with perforated plate spargers. Chem. Eng. Process. **70**, 259–266 (2013)
7. Sokolichin, A., Eigenberger, G.: Gas–liquid flow in bubble columns and loop reactors: part I. Detailed modelling and numerical simulation. Chem. Eng. Sci. **49**, 5735–5746 (1994)
8. Kumar, A., Degaleesan, T., Laddha, G., Hoelscher, H.: Bubble swarm characteristics in bubble columns. Can. J. Chem. Eng. **54**, 503–508 (1976)
9. Rezakazemi, M.: CFD simulation of seawater purification using direct contact membrane desalination (DCMD) system. Desalination **443**, 323–332 (2018)
10. Hajilary, N., Rezakazemi, M.: CFD modeling of CO2 capture by water-based nanofluids using hollow fiber membrane contactor. Int. J. Greenhouse Gas Control **77**, 88–95 (2018)
11. Besagni, G., Guédon, G.R., Inzoli, F.: Annular Gap Bubble Column: experimental Investigation and Computational Fluid Dynamics Modeling. J. Fluids Eng. **138**, 011302 (2016)
12. Rzehak, R., Krepper, E.: CFD modeling of bubble-induced turbulence. Int. J. Multiph. Flow **55**, 138–155 (2013)
13. Rezakazemi, M., Shirazian, S.: Gas-liquid phase recirculation in bubble column reactors: development of a hybrid model based on local CFD—Adaptive Neuro-Fuzzy Inference System (ANFIS). J. Non-Equilib. Thermodyn **44**. 29–42 (2019)
14. Tabib, M.V., Roy, S.A., Joshi, J.B.: CFD simulation of bubble column—an analysis of interphase forces and turbulence models. Chem. Eng. J. **139**, 589–614 (2008)
15. Rezakazemi, M., Shirazian, S.: Development of a 3D hybrid intelligent-mechanistic model for simulation of multiphase chemical reactors. Chem. Eng. Technol. **41**, 1982–1993 (2018)
16. Sokolichin, A., Eigenberger, G., Lapin, A.: Simulation of buoyancy driven bubbly flow: established simplifications and open questions. AIChE J. **50**, 24–45 (2004)
17. McClure, D.D., Aboudha, N., Kavanagh, J.M., Fletcher, D.F., Barton, G.W.: Mixing in bubble column reactors: experimental study and CFD modeling. Chem. Eng. J. **264**, 291–301 (2015)
18. Liu, Y., Hinrichsen, O.: Study on CFD–PBM turbulence closures based on k–ε and Reynolds stress models for heterogeneous bubble column flows. Comput. Fluids **105**, 91–100 (2014)
19. Joshi, J.: Computational flow modelling and design of bubble column reactors. Chem. Eng. Sci. **56**, 5893–5933 (2001)
20. Qiu, J., Sun, K., Wang, T., Gao, H.: Observer-based fuzzy adaptive event-triggered control for pure-feedback nonlinear

systems with prescribed performance. IEEE Trans. Fuzzy Syst. (2019). https://doi.org/10.1109/TFUZZ.2019.2895560
21. Sun, K., Mou, S., Qiu, J., Wang, T., Gao, H.: Adaptive fuzzy control for non-triangular structural stochastic switched nonlinear systems with full state constraints. IEEE Trans. Fuzzy Syst. **27**, 1587–1601 (2018)
22. Rostamizadeh, M., Rezakazemi, M., Shahidi, K., Mohammadi, T.: Gas permeation through H_2-selective mixed matrix membranes: experimental and neural network modeling. Int. J. Hydrog. Energy **38**, 1128–1135 (2013)
23. Rezakazemi, M., Mohammadi, T.: Gas sorption in H_2-selective mixed matrix membranes: experimental and neural network modeling. Int. J. Hydrog. Energy **38**, 14035–14041 (2013)
24. Soroush, E., Mesbah, M., Hajilary, N., Rezakazemi, M.: ANFIS modeling for prediction of CO_2 solubility in potassium and sodium based amino acid Salt solutions. J. Environ. Chem. Eng. **7**, 102925 (2019)
25. Rezakazemi, M., Mosavi, A., Shirazian, S.: ANFIS pattern for molecular membranes separation optimization. J. Mol. Liq. **274**, 470–476 (2019)
26. Dashti, A., Harami, H.R., Rezakazemi, M.: Accurate prediction of solubility of gases within H_2-selective nanocomposite membranes using committee machine intelligent system. Int. J. Hydrog. Energy **43**, 6614–6624 (2018)
27. Jang, J.-S.: ANFIS: adaptive-network-based fuzzy inference system. IEEE Trans. Syst. Man Cybern. **23**, 665–685 (1993)
28. Lei, Y., He, Z., Zi, Y., Hu, Q.: Fault diagnosis of rotating machinery based on multiple ANFIS combination with GAs. Mech. Syst. Signal Process. **21**, 2280–2294 (2007)
29. K.C. Schurter, P.N. Roschke,: In: The Ninth IEEE International Conference on Fuzzy modeling of a magnetorheological damper using ANFIS, Fuzzy Systems, 2000. FUZZ IEEE 2000, pp. 122–127. IEEE, New York (2000)
30. Rezakazemi, M., Dashti, A., Asghari, M., Shirazian, S.: H_2-selective mixed matrix membranes modeling using ANFIS, PSO-ANFIS, GA-ANFIS. Int. J. Hydrog. Energy **42**, 15211–15225 (2017)
31. Yilmaz, I., Kaynar, O.: Multiple regression, ANN (RBF, MLP) and ANFIS models for prediction of swell potential of clayey soils. Expert Syst. Appl. **38**, 5958–5966 (2011)
32. Jang, J.-S.R., Sun, C.-T., Mizutani, E.: Neuro-fuzzy and soft computing; a computational approach to learning and machine intelligence, (1997)
33. Yun, Z., Quan, Z., Caixin, S., Shaolan, L., Yuming, L., Yang, S.: RBF neural network and ANFIS-based short-term load forecasting approach in real-time price environment. IEEE Trans. Power Syst. **23**, 853–858 (2008)
34. Pourtousi, M., Ganesan, P., Sahu, J., Redzwan, G.: Sensitivity study of Bubble diameter for prediction of flow pattern in homogeneous bubble column regime, IOP Conference Series: Materials Science and Engineering, IOP Publishing, pp. 012004 (2015)
35. Azwadi, C.S.N., Zeinali, M., Safdari, A., Kazemi, A.: Adaptive-network-based fuzzy inference system analysis to predict the temperature and flow fields in a lid-driven cavity. Numer. Heat Transf. Part A: Appl. **63**, 906–920 (2013)
36. Jang, J.-S.: Proceedings of the Fifth IEEE International Conference on Input Selection for ANFIS Learning, Fuzzy Systems, 1996, pp. 1493–1499. IEEE, New York (1996)
37. Pfleger, D., Becker, S.: Modelling and simulation of the dynamic flow behaviour in a bubble column. Chem. Eng. Sci. **56**, 1737–1747 (2001)
38. de Bertodano, M.A.L.: Turbulent bubbly two-phase flow in a triangular duct. Dissertation, (1992)
39. Laborde-Boutet, C., Larachi, F., Dromard, N., Delsart, O., Schweich, D.: CFD simulation of bubble column flows: investigations on turbulence models in RANS approach. Chem. Eng. Sci. **64**, 4399–4413 (2009)
40. Cevik, A., Sezer, E.A., Cabalar, A.F., Gokceoglu, C.: Modeling of the uniaxial compressive strength of some clay-bearing rocks using neural network. Appl. Soft Comput. **11**, 2587–2594 (2011)
41. Avila, G., Pacheco-Vega, A.: Fuzzy-C-means-based classification of thermodynamic-property data: a critical assessment. Numer. Heat Transf. Part A: Appl. **56**, 880–896 (2009)
42. Mahmoud, M.A., Ben-Nakhi, A.E.: Neural networks analysis of free laminar convection heat transfer in a partitioned enclosure. Commun. Nonlinear Sci. Numer. Simul. **12**, 1265–1276 (2007)
43. Salehi, H., Zeinali-Heris, S., Esfandyari, M., Koolivand, M.: Nero-fuzzy modeling of the convection heat transfer coefficient for the nanofluid. Heat Mass Transf. **49**, 575–583 (2013)
44. Ryoo, J., Dragojlovic, Z., Kaminski, D.A.: Control of convergence in a computational fluid dynamics simulation using ANFIS. IEEE Trans. Fuzzy Syst. **13**, 42–47 (2005)
45. Rezakazemi, M., Azarafza, A., Dashti, A., Shirazian, S.: Development of hybrid models for prediction of gas permeation through FS/POSS/PDMS nanocomposite membranes. Int. J. Hydrog. Energy **43**, 17283–17294 (2018)
46. Dashti, A., Riasat Harami, H., Rezakazemi, M., Shirazian, S.: Estimating CH_4 and CO_2 solubilities in ionic liquids using computational intelligence approaches. J. Mol. Liq. **271**, 661–669 (2018)
47. Dashti, A., Asghari, M., Dehghani, M., Rezakazemi, M., Mohammadi, A.H., Bhatia, S.K.: Molecular dynamics, grand canonical Monte Carlo and expert simulations and modeling of water–acetic acid pervaporation using polyvinyl alcohol/tetraethyl orthosilicates membrane. J. Mol. Liq. **265**, 53–68 (2018)
48. Rezakazemi, M., Ghafarinazari, A., Shirazian, S., Khoshsima, A.: Numerical modeling and optimization of wastewater treatment using porous polymeric membranes. Polym. Eng. Sci. **53**, 1272–1278 (2012)
49. Ben-Nakhi, A., Mahmoud, M.A., Mahmoud, A.M.: Inter-model comparison of CFD and neural network analysis of natural convection heat transfer in a partitioned enclosure. Appl. Math. Model. **32**, 1834–1847 (2008)
50. Aminossadati, S., Kargar, A., Ghasemi, B.: Adaptive network-based fuzzy inference system analysis of mixed convection in a two-sided lid-driven cavity filled with a nanofluid. Int. J. Therm. Sci. **52**, 102–111 (2012)
51. Pourtousi, M.: CFD modelling and ANFIS development for the hydrodynamics prediction of bubble column reactor ring sparger. Dissertation, University of Malaya (2016)
52. Pourtousi, M., Sahu, J., Ganesan, P., Shamshirband, S., Redzwan, G.: A combination of computational fluid dynamics (CFD) and adaptive neuro-fuzzy system (ANFIS) for prediction of the bubble column hydrodynamics. Powder Technol. **274**, 466–481 (2015)
53. Pourtousi, M., Zeinali, M., Ganesan, P., Sahu, J.: Prediction of multiphase flow pattern inside a 3D bubble column reactor using a combination of CFD and ANFIS. RSC Adv. **5**, 85652–85672 (2015)
54. Babanezhad, M., Rezakazemi, M., Hajilary, N., Shirazian, S.: Liquid-phase chemical reactors: development of 3D hybrid model based on CFD-adaptive network-based fuzzy inference system. Can. J. Chem. Eng. **97**, 1676–1684 (2019)

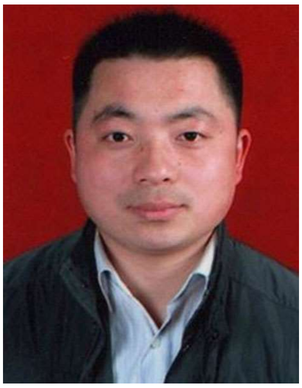

Erlin Tian received his M.Sc. degree in 2008 from the HuaZhong University of Science and Technology, China in Wuhan. He is an A.P., in the School of ZhengZhou University of Light Industry, China. His research interests include high-precision time-frequency measurement, signal detection, and processing.

Meisam Babanezhad received his M.Sc. degree in Operation Energy conversion from the Islamic Azad University of South Tehran branch, Iran in 2019. His research interests include artificial intelligence, optimization algorithm, Deep learning, machine learning, and CFD.

Dr. Mashallah Rezakazemi received his BSc. and MSc. degrees in 2009 and 2011, respectively, both in Chemical Engineering, from the Iran University of Science and Technology (IUST), and his Ph.D. from the University of Tehran (UT) in 2015. Ever since his first appointment in 2016, Rezakazemi has serving as an assistant professor of the Faculty of Chemical and Materials Engineering at the Shahrood University of Technology. Dr. Rezakazemi's research is focused on the general area of the water–energy nexus, CO2 capture, gas separation, desalination, process simulation, and fluid dynamics.

Dr. Saeed Shirazian is Visiting Researcher at the Faculty of Applied Sciences, Ton Duc Thang University, Vietnam. He received his Ph.D in Chemical Engineering from the Iran University of Science and Technology (IUST). His research interests include process engineering, process modeling and simulation, pharmaceutical manufacturing, and separation.